Available online at www.sciencedirect.com
ScienceDirect
Polymer 48 (2007) 4793–4803
polymer
www.elsevier.com/locate/polymer

Effects of aggregation structure on rheological properties of thermoplastic polyurethanes

Satoshi Yamasaki [a,c], Daisuke Nishiguchi [c], Ken Kojio [b], Mutsuhisa Furukawa [a,*]

[a] Department of Materials Science, Graduate School of Science and Technology, Nagasaki University, 1-14 Bunkyo-machi, Nagasaki 852-8521, Japan
[b] Department of Materials Science and Engineering, Faculty of Engineering, Nagasaki University, 1-14 Bunkyo-machi, Nagasaki 852-8521, Japan
[c] R&D Center, Mitsui Chemicals Polyurethanes, Inc., 580-32 Nagaura, Sodegaura, Chiba 299-0265, Japan

Received 14 February 2007; received in revised form 26 May 2007; accepted 6 June 2007
Available online 9 June 2007

Abstract

The effects of the molecular aggregation structure on the rheological properties of thermoplastic polyurethane (TPU) were investigated. The TPU was composed of poly{(tetramethylene adipate)-*co*-(hexamethylene adipate)} glycol as the soft segments, 4,4′-diphenylmethane diisocyanate and 1,4-butanediol as the hard segments. The TPU sheets prepared by injection molding were annealed at various temperatures from 23 to 120 °C to vary the molecular aggregation structure. Glass transition temperature of the soft segment and melting points of the hard segment domains of the TPUs decreased and increased, respectively, with increasing annealing temperature. The results of DSC, solid-state NMR spectroscopy and dynamic viscoelastic measurements revealed that the degree of micro-phase separation of the TPUs becomes stronger with increasing annealing temperature due to the progress of formation of well-organized hard segment domains. The dynamic temperature sweep experiments for molten TPUs revealed that the temperature at critical gel point, which is defined as the temperature at which the dynamic storage modulus coincides with the loss storage modulus, in the cooling process increased with the progress of aggregation of the hard segments in the TPUs observed in the solid state. The uniaxial elongational viscosity measurements showed that TPUs exhibited an obvious strain hardening behavior with strain rate owing to residual hard segment domains at an operating temperature. It was revealed that the formation of well-organized hard segment domains had a profound effect on the rheological properties of TPUs, in particular on their elongational viscosity.

Keywords: Thermoplastic polyurethanes; Rheological properties; Strain hardening

1. Introduction

Thermoplastic polyurethanes (TPUs) are high performance elastomers with applications as coating, fibers, films, footwear, wire and flexible tubing [1,2]. TPUs are multi-block copolymers consisting of hard and soft segments, produced by polyaddition reaction of a diisocyanate with linear polymer glycols and a low molecular weight diol as a chain extender. The thermodynamic incompatibility of these segments drives their micro-phase separation into hard and soft segment phases.

Thermal history, various deformations and annealing after the polymer processing greatly affect the micro-aggregation structure and properties of TPUs. There are many studies [3–12] on the thermal properties and the micro-aggregation structure of MDI–BD-based TPUs investigated by differential scanning calorimetry (DSC), small angle X-ray scattering (SAXS), wide angle X-ray diffraction (WAXD) and infrared spectroscopy (IR). In contrast, the rheological properties of MDI–BD-based TPUs have not been the subject of intensive study [13–16], although there are some reports on the effects of structure of aliphatic diisocyanate based TPUs on their rheological properties [17–19] and on the melt rheology of segmented non-chain extended polyureas [20].

Velankar et al. studied the rheological properties of polyurethane melts [17–19]. They claimed that the primary reason

* Corresponding author. Tel.: +81 95 819 2650; fax: +81 95 819 2651.
E-mail addresses: satoshi.yamasaki@mitsui-chem.co.jp (S. Yamasaki), daisuke.nishiguchi@mitsui-chem.co.jp (D. Nishiguchi), kojio@nagasaki-u.ac.jp (K. Kojio), furukawa@nagasaki-u.ac.jp (M. Furukawa).

0032-3861/$ - see front matter © 2007 Elsevier Ltd. All rights reserved.
doi:10.1016/j.polymer.2007.06.006

for the reduced number of studies on the rheological properties of TPUs was instability of the aromatic urethane linkage at molten phase, which did not allow long-duration melt experiments. Thus, they selected aliphatic TPUs, which are likely to be stable at high temperature, to characterize the rheological properties in detail.

Recently, Yoon and Han [13] investigated the effect of thermal history on the rheological behavior of ester- and ether-based commercial TPUs composed of MDI and BD, and they showed that the injection molding temperature for specimen preparation had a profound influence on the variation of dynamic storage and loss moduli (G' and G'') and the state of hydrogen bonding with time. Hentschel et al. [14] studied the kinetics of molar mass decrease in the molten state of an MDI–BD-based TPU using dynamic melt viscometry measurement. They revealed that the temperature dependence of the zero shear viscosity was affected not only by the molecular mobility but also by the change in molecular weight due to urethane exchange reaction. Lu et al. [15] used three different apparatuses, which were a dynamic shear, a capillary rheometry and an instrumented batch mixer to investigate the effect of degradation during TPU processing on the melt viscosity and reported the apparent activation energy of flow (E_a) and true activation energy of flow (E_η) were 328 and 144 kJ/mol, respectively. Their equation to calculate the contribution of flow and the degradation reaction of TPU to overall activation energy was as follows: $E_a = E_\eta + 1.7 \times \Delta H_{deg}$. More recently, Cossar et al. [16] investigated the phase transition behavior of a commercial MDI- and BD-based TPU by rheological techniques and revealed that the micro-phase separation between hard and soft segments and the concurrent crystallization of hard phase domains produced a sol-to-gel type of transition and the microstructure of TPUs at the critical gel point was strictly related to the thermal history.

These experimental results show that the both micro-phase-separated structure and rheological properties of TPUs are strongly affected by the degradation reaction in the melt state and their thermal history during processing. However, comparatively little information has emerged on the effects of the micro-phase separation structure on the rheological properties of TPUs. In particular, no results, to our knowledge, have ever been reported on the effect of the micro-phase separation structure on the elongational viscosity. The extensional flow is very popular in polymer processing operations, and well known to supply information not only on the molecular mobility but also on the polymer processing operations related to film casting, tubular film inflation, film stretch, fiber spinning and blow molding, etc. Thus, it is indispensable to clarify the relationship between the molecular aggregation structure and rheological properties of MDI–BD-based TPUs from the viewpoint of polymer processing.

The purpose of this work is to clarify the effects of the molecular aggregation structure on the rheological properties of TPUs. The poly (ester-polyol), MDI- and BD-based TPUs prepared by injection molding were annealed at various temperatures to vary the molecular aggregation structure. The molecular aggregation structures of TPUs were investigated by DSC, solid-state NMR and dynamic viscoelastic measurement. The rheological properties of TPU melts were evaluated using a rotational type rheometer in oscillatory mode and a Meissner type uniaxial extensional rheometer.

2. Experimental

2.1. Materials and sample preparation

The TPU used in this study was Elastollan® C85A-10 (BASF Japan Co. Ltd., Japan). The TPU sheets were prepared using the procedures described below. As-received TPU pellets were dried under reduced pressure at 90 °C for 24 h. The TPU sheets were prepared using an injection molding machine (Meiki Seisakusyo, model M100A II-DH, Japan) with a screw diameter of 40 mm, and three zones to control barrel temperature. The zones' temperature was set to 180, 200 and 200 °C, respectively, and the nozzle temperature was set to 200 °C. The mold size was 200 mm in length, 150 mm in width and 2 mm in thickness and the temperature was maintained at 30 °C. The holding time was 30 s and injection pressure was 200 MPa. To obtain four specimens with different micro-aggregation structures, the TPU sheets were annealed, immediately after injection molding, in an oven at 23, 80, 100 and 120 °C for 4 h, respectively. The relative humidity in an oven at 23 °C was controlled at 55%. After annealing, specimens were stored at 23 °C and 55% relative humidity for one week in an oven. In addition, the TPU pellets were annealed under the same condition as the sheets, and then stored at 23 °C and 55% relative humidity for one week in an oven to measure the density of the TPUs using a pressure–volume–temperature apparatus. The nomenclature of the specimens denotes poly(ester-polyol) of the soft segments (ES), hardness of the TPU mentioned in the catalog (85) and annealing temperature (23, 80, 100, 120), for example ES-85-23.

2.2. Characterization

2.2.1. Gel permeation chromatography (GPC)

The molecular weight and the molecular weight distribution of the TPU sheets were measured using GPC (model HLC-8220GPC, Tosoh, Japan) equipped with three different columns (Shodex GPC column KD-804, KD-8025, and KD-802, Showa Denko, Japan), and an ultraviolet detector (wave length 264 nm). Polystyrenes with different molecular weights were used as standards. The mobile phase was *N*,*N*-dimethylformamide (DMF) with dissolved LiBr at 0.01 mol L^{-1} at a flow rate of 0.6 ml min^{-1}, and the column temperature was maintained at 40 °C.

2.2.2. Nuclear magnetic resonance spectroscopy (NMR)

^1H and ^{13}C NMR experiments were performed using a FT-NMR (model ECP-500, JEOL) spectrometer at 60 °C to determine the chemical structure of as-received TPU pellets. ^1H NMR spectroscopy was done by the single pulsed method at 500 Hz with 128 scans. The pellets were dissolved in deuterated dimethyl sulfoxide (DMSO) as 4% w/v solution, after

drying them at 70 °C for 2 h under reduced pressure. On the other hand, ^{13}C NMR spectroscopy was done using the single pulsed decoupling method at 125 MHz with 6000 scans, using a TPU solution of 20% w/v in deuterated DMSO, after drying the pellets under the same condition described above.

2.2.3. Differential scanning calorimetry (DSC)

The thermal behavior of the TPU sheets was determined using DSC (model SSC5200/SSC5200H, Seiko Instruments Inc., Japan). DSC thermograms were obtained at temperatures ranging from −90 to 230 °C with a heating rate of 10 °C min^{-1} under a nitrogen atmosphere. Each sample was cooled at −100 °C and after being held at −100 °C for 10 min, measurements were carried out up to 270 °C. The sample weighed 8–10 mg and indium was used to calibrate the DSC cell constant. To determine the start temperature for re-crystallization of the hard segments ($T_{c,\ start}$) in the TPU sheets, DSC thermograms were obtained during the cooling process from 215 to 25 °C after heating to 215 °C at heating and cooling rates of 10 °C min^{-1} under a nitrogen atmosphere.

2.2.4. Solid-state nuclear magnetic resonance spectroscopy (NMR)

Solid-state NMR spectroscopy of the TPU sheets was performed in an FT-NMR (model MU25, JEOL, Japan) spectrometer operating at 25 MHz for ^{1}H at 40 °C. ^{1}H 90° pulse width was set to 2.0 μs while the number of scans was typically 16. The measurement temperature was controlled using a JEOL MU25 temperature-controlling unit. The free induction decay (FID) curve was measured using a solid echo method. The relative proton content and the spin–spin relaxation time (T_2) of each decay component were calculated using a device equipped with a software, based on non-linear least squares regression to the FID curve acquired. The FID curve was separated into three decay components [20]. The fast decay component, the intermediate decay between fast and slow decays and the slow decay component were fitted to a Gaussian function, an exponential function and an exponential function, respectively.

2.2.5. Dynamic viscoelastic properties

The temperature dependence of the dynamic viscoelastic properties of TPU sheets was measured using a Rheometrics mechanical spectrometer (model RSA II, Rheometrics Scientific, USA) at temperatures ranging from −80 to 200 °C, at a heating rate of 3 °C min^{-1} and a frequency of 1 Hz under a nitrogen atmosphere.

2.2.6. Density measurement

For the analysis of experimental data of uniaxial elongational viscosity, the densities of the TPU at measurement temperatures (175, 180 and 190 °C) were necessary. The pressure–volume–temperature (PVT) properties of TPU pellets, annealed under the conditions described above, were measured by cooling from the melt state under various constant pressures using an apparatus for PVT measurement (model PVT-100, SWO Polymertechnik GmbH, Germany) to obtain the specific volume of TPUs. Before PVT measurements, all pellets were dried at 70 °C for 2 h under reduced pressure. The pellets were heated to 230 °C and cooled to 25 °C at a cooling rate of 5 °C min^{-1} at 20, 60 and 100 MPa in the apparatus. The specific volumes at 25, 175, 180 and 190 °C at 0.1 MPa, estimated by using a device equipped with software, were converted into the density at these temperatures.

2.2.7. Rheological properties

Rheological measurements of TPU sheets were carried out on a stress-controlled rheometer (model SR-5000, Rheometrics Scientific) equipped with a cone and plate fixture of 25 mm diameter for the plate and 0.1 rad (0.57°) cone angle. All rheological measurements were conducted under a nitrogen atmosphere to prevent oxidative degradation of the specimens. Before rheological measurements, all specimens were cut into a disk or rectangular card shape, and then they were dried at 70 °C for 1.5 h under a reduced pressure to prevent interference by moisture in the specimens. Dynamic temperature sweep experiments during both the heating and cooling processes, using the same specimen, were conducted at a frequency of 0.628 rad s^{-1} and an initial stress of 100 Pa within the linear viscoelastic region. The specimen was placed in the cone and plate fixture of the rheometer that had been heated to 180 °C and held there for 3 min to prevent slippage, and then the gap was set to ca. 0.056 mm in all the runs. Three minutes were required to load due to reduction of the normal stress of the specimen occurring while adjusting the gap. The specimen was heated up to 215 °C and then cooled to ca. 130 °C at heating and cooling rates of 3 °C min^{-1}, without holding at 215 °C. It took ca. 38 min during both the heating and cooling processes.

Dynamic time sweep experiments of ES-85-23 were conducted at an initial stress of 100 Pa at temperatures ranging from 180 to 225 °C. Measurement at each temperature took 50 min (3000 s). The frequencies were set to be 0.314 rad s^{-1} at 180 and 190 °C, and 0.628 rad s^{-1} at 195, 205, 215 and 225 °C. The cone and plate were preheated same as in dynamic temperature sweep experiments described above. The loading time, which differed depending on the given temperature, was 2–4 min after preheating on the rheometer. Immediately after the dynamic time sweep experiments, the specimens were removed from the rheometer in the molten liquid state and dissolved in DMF solution with 0.5% w/v di-*n*-butyl amine to avoid any crosslink reactions. The M_w values of these specimens were measured by GPC as described above to check for thermal stability.

Dynamic frequency sweep experiments were conducted at 0.1–100 rad s^{-1} from 175 to 215 °C. The gap was set to ca. 0.056 mm in all runs. The data acquisitions at 175, 180 and 185 °C were started at 6–10 min after the sample was mounted on the rheometer, while those at 195, 205, and 215 °C began 3 min after the sample was mounted.

Uniaxial elongational viscosity was measured on a Meissner type rheometer (model RME, Rheometrics Scientific) with a strain speed ranging from 0.01 to 1.0 s^{-1} at 175, 180 and 190 °C. The strain dependence of uniaxial elongational viscosity of the TPU sheets was measured at each temperature. All measurements were conducted under a nitrogen atmosphere

to prevent oxidative degradation of the specimens. A specimen 100 mm in length and 7 mm in width was cut from the sheet and quickly placed on the geometry in the rheometer that had been heated to a given temperature and held there for 3.5, 3 and 1 min at 175, 180 and 190 °C, respectively, to prevent slippage and slackness of the specimen on the geometry.

3. Results and discussion

Table 1 shows the number-average molecular weight (M_n), the weight-average molecular weight (M_w) and the molecular weight distribution for ES-85-23, -80, -100 and -120. M_n and M_w of as-received TPU pellets were 35.0×10^3 and 197.0×10^3, respectively. Thus, M_ns and M_ws of all TPU sheets prepared by injection molding decreased owing to a strong shear stress during their processing. The deviations of M_n and M_w for all sheets were within ±5%. M_ns and M_ws for all sheets exhibited almost the same values, although those of ES-85-23 were slightly higher than the others. Since these TPU sheets subjected to annealing treatment could be dissolved in DMF, it seems that they were linear that had scarcely any allophanate crosslinks.

Its composition was determined by ^{1}H and ^{13}C NMR spectroscopies. This TPU is composed of MDI and BD as the hard segment, and poly{(tetramethylene adipate)-*co*-(hexamethylene adipate)} glycol as the soft segment. The content of MDI and BD was determined as 14 and 13 mol%, respectively. On the other hand, the content of each monomer in poly{(tetramethylene adipate)-*co*-(hexamethylene adipate)} glycol was determined as follows: BD, 1,6-hexanediol and adipic acid were 23, 14 and 36 mol%, respectively. We confirmed that TPU did not contain any fillers.

The thermal properties of the TPU sheets were investigated using DSC. Fig. 1 shows the DSC thermograms for ES-85-23, -80, -100 and -120. Table 2 shows the glass transition temperature (T_g) of the soft segments, and the ΔT_g, heat capacity (ΔC_p) at the glass transition region and melting point ($T_{m,hi}$) of the hard segment domains of the TPUs. ΔT_g corresponds to the transition width of glass transition. $T_{m,hi}$ $(i=1,2,3)$ were simply defined as $T_{m,h1}$,$T_{m,h2}$ and $T_{m,h3}$ from the lower temperature side. T_gs of the soft segments and ΔC_p at the glass transition region decreased ca. 7 °C and increased ca. 0.02 J/g K with increasing annealing temperature. In addition, ΔT_g decreased with increasing annealing temperature, respectively. These results clearly indicate that the degree of micro-phase separation became stronger with increasing annealing temperature. On the other hand, $T_{m,h2}$ and $T_{m,h3}$ did not depend on the annealing temperature, while $T_{m,h1}$ markedly increased with increasing annealing temperature. $T_{m,h1}$ values were 20–40 °C higher than the annealing temperature and these increases of $T_{m,h1}$ corresponded well with the experimental results reported by Seymour et al. [3] and Hesketh et al. [11]. Based on the fact that the melting point for the hard segment model polyurethane was 194 [22] or 208 °C [23] and the TPUs are multi-block polymers, the $T_{m,h2}$ observed around ca. 161 °C might be attributed to melting of the disordered hard segment domains formed with hydrogen bonds, where the degree of aggregation of the hard segments was slightly higher than that observed as $T_{m,h1}$. In contrast, the $T_{m,h3}$ values observed around ca. 180 °C were attributed to melting of the well-organized hard segment domains.

Table 1
Average molecular weight and molecular weight distribution[a]

	$M_n \times 10^{-3}$ (g/mol)	$M_w \times 10^{-3}$ (g/mol)	M_w/M_n
ES-85-23	30.8	180.3	5.86
ES-85-80	27.4	151.5	5.54
ES-85-100	26.5	151.6	5.76
ES-85-120	28.5	152.9	5.37

[a] Molecular weight of TPU sheets is determined by GPC in 0.01 mol L^{-1} LiBr–DMF solution at a column temperature of 40 °C using polystyrene standards for calibration.

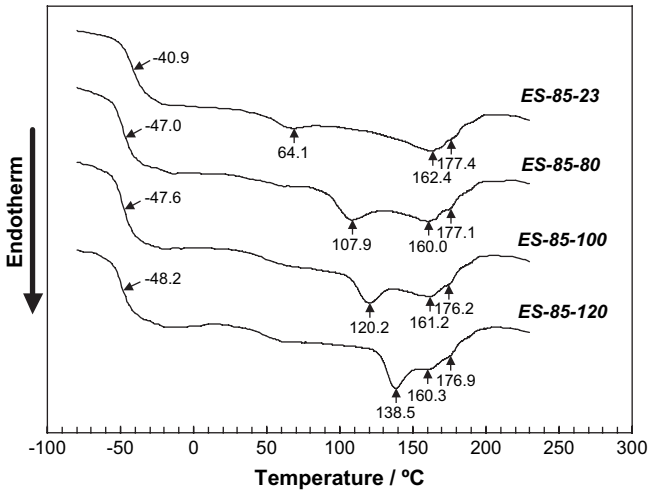

Fig. 1. DSC thermograms for ES-85-23, -80, -100 and -120.

Solid-state NMR measurements were carried out to evaluate the spin–spin relaxation times and the relative proton content of each phase for the TPU sheets at 40 °C. First, we tried to separate the FID curve into two components [24]. The fast decay component and the slow decay component were fitted to a Gaussian function and an exponential function, respectively. However, the calculated curves did not fit with the experimental results. We added another Lorentzian function [21] as follows:

$$M(t) = M(t_f)\exp\left(-\frac{t^2}{T_{2f}^2}\right) + M(t_i)\exp\left(-\frac{t}{T_{2i}}\right) + M(t_s)\exp\left(-\frac{t}{T_{2s}}\right) \quad (1)$$

Where, $M(t_f)$ and $M(t_s)$ represent the initial values of normalized magnetization of fast and slow decay, respectively, and T_{2f} and T_{2s} are the spin–spin relaxation time of the corresponding components. The fast decay component was attributed to the hard segment phase, in which the molecular mobility was constrained by the aggregation of the hard segment, while the slow decay component was attributed to the soft segment phase, in which the mobility was high. $M(t_i)$ represents the initial values of normalized magnetization of an

Table 2
Thermal properties[a] of TPU sheets

Sample code	$T_{g,\ start}$ (°C)	T_g (°C)	$T_{g,\ end}$[b] (°C)	ΔT_g[c]	ΔC_p[d] (J/g K)	$T_{m,h1}$ (°C)	$T_{m,h2}$ (°C)	$T_{m,h3}$[e] (°C)
ES-85-23	−49.6	−40.9	−31.8	17.8	0.395	64.1	162.4	177.4
ES-85-80	−53.9	−47.0	−38.6	15.3	0.405	107.9	160.0	177.1
ES-85-100	−54.2	−47.6	−39.8	14.4	0.411	120.2	161.2	176.2
ES-85-120	−55.2	−48.2	−41.4	13.8	0.412	138.5	160.3	176.9

[a] Thermal properties are measured by DSC in the temperatures ranging from −100 to 270 °C with a heating rate of 10 °C min^{-1} under a nitrogen atmosphere.
[b] Glass transition temperatures of the soft segments.
[c] ΔT_g was calculated by $T_{g,\ end} - T_{g,\ start}$.
[d] Heat capacity at glass transition region.
[e] $T_{m,hi(i=1,2,3)}$ are melting points of the hard segment domains.

intermediate decay between fast and slow decays and T_{2i} is the spin−spin relaxation time of the component. The intermediate decay component was attributed to the interfacial phase, which was mainly composed of soft segments constrained by the hard segments. Eq. (1) that included three decay components was a good approximation for all TPU sheets. By applying a non-linear least squares fit to the FID signals acquired, we could obtain T_{2f}, T_{2i} and T_{2s} and the relative proton content of each decay component ($M(t_f)$, $M(t_i)$ and $M(t_s)$).

Fig. 2 shows the annealing temperature dependence of the spin−spin relaxation times (T_{2f}, T_{2i} and T_{2s}) and the relative proton content of fast, intermediate and slow decay components for ES-85-23, -80, -100 and -120. The T_{2f}, T_{2i} and T_{2s} for the TPU sheets were separated into three values, ca. 20–23 μs, ca. 260–320 μs and ca. 690–720 μs, respectively. Firstly, T_{2f} decreased and T_{2i} and T_{2s} increased with increasing annealing temperature. These results imply that the hard and soft segment phases became richer with increasing annealing. Secondly, the relative proton content of the T_{2f} and T_{2i} components decreased and that of the T_{2s} component increased with increasing annealing temperature. It seems that the T_{2i} component, which decreased from ca. 0.65 to ca. 0.61, mainly changed to the T_{2s} component. Thus, the TPUs have a strong micro-phase separated structure with increasing annealing temperature as shown by DSC.

Fig. 3 shows the temperature dependence of the dynamic storage modulus (E') and loss tangent (tan δ) for ES-85-23, -80, -100 and -120. Abrupt decreasing E' and α-relaxation peak from glass transition of soft segment were observed at around −30 °C. The temperature dependence (slope) of E' observed from ca. −50 to ca. −10 °C increased and the α-relaxation peak of tan δ shifted to lower temperature with increasing annealing temperature. These results suggested that the mobility of the soft segments increased with increasing annealing temperature due to a formation of purer phases. In addition, E' values at 23 °C decreased from 25.6 MPa for the ES-85-23 to 15.6 MPa for the ES-85-120, whereas the termination temperature of the rubbery plateau region increased from 48.2 °C for the ES-85-23 to 132.6 °C for the ES-85-120 with increasing annealing temperature. These results can be attributed to a decrease of the physical crosslink density because of the formation of a small amount of well-organized hard segment domains. In particular, the decrease of the physical crosslink density was related to a decrease of the content of the hard segment phase, as shown by solid-state NMR. Thus, these results suggest that the soft

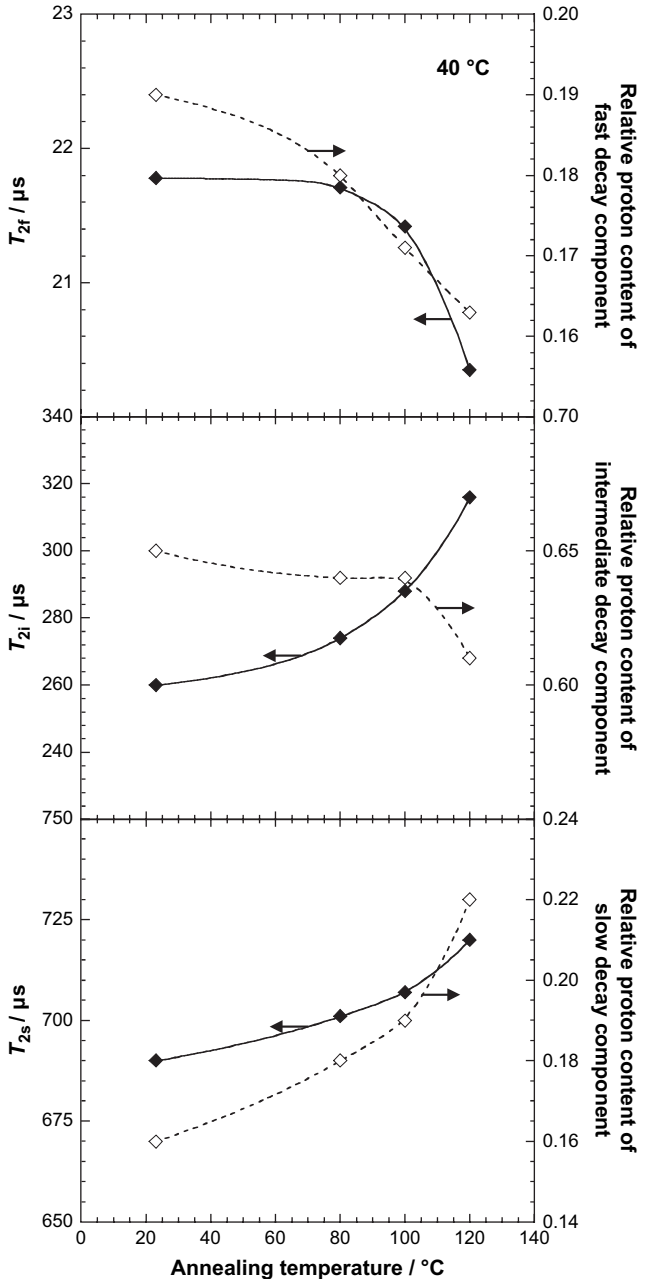

Fig. 2. Annealing temperature dependence of the spin−spin relaxation times (T_{2f}, T_{2i}, T_{2s}) of the corresponding fast, intermediate and slow decay components and the relative proton content of the three decay components.

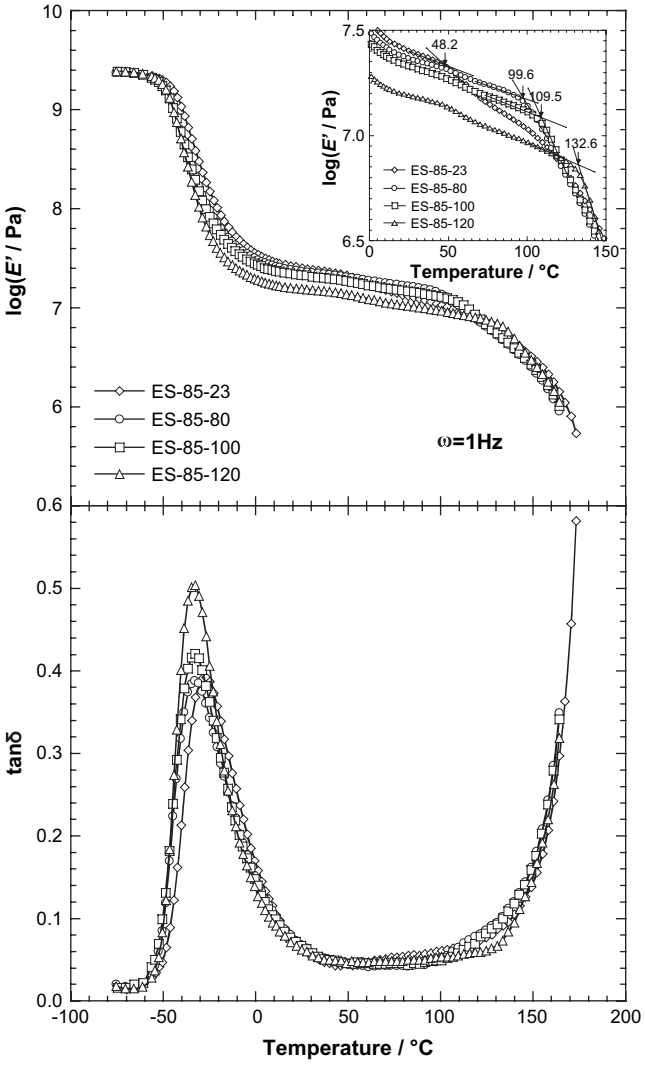

Fig. 3. Temperature dependence of the dynamic storage modulus (E') and loss tangent (tan δ) for ES-85-23, -80, -100 and -120.

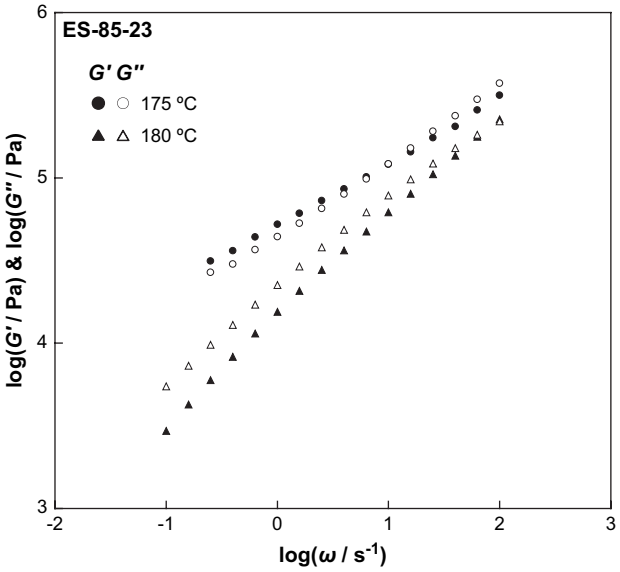

Fig. 4. Frequency dependence of the dynamic storage modulus (G') and dynamic loss modulus (G'') at 175 and 180 °C of ES-85-23.

segment components mixed in or around the hard segment phases were segregated and the content of the hard segment and the interfacial phases decreased. In addition, the termination temperature of the rubbery plateau region increased due to an increasing molecular packing of the hard segments. From the results of DSC, pulsed NMR and dynamic viscoelastic measurements, it is conceivable that the degree of micro-phase separation between the soft and hard segments became stronger in the TPUs with increasing annealing temperature due to the progress of formation of well-organized hard segment domains.

The rheological properties of TPUs were investigated using a stress-controlled rheometer. Fig. 4 shows the frequency dependence of G' and G'' at 175 and 180 °C for ES-85-23. G' values were almost same as G'' ones at 175 °C, in contrast G'' values were larger than G' ones at 180 °C. These trends were observed for all TPUs in frequency sweep tests above 180 °C. Thus, TPUs were in the sol–gel transition state at 175 °C and in the melt state at 180 °C. We chose 180 °C as the start temperature for the temperature sweep experiments. Usually, TPUs are extruded at temperatures ranging from 175 to 215 °C [1] and then gradually cooled to around room temperature to produce films, sheets, tubes, fibers, etc. Hence, the investigation of the rheological properties in the heating and cooling processes is important for polymer processing operations. Fig. 5 shows the temperature dependence of G' and G'' during both the heating and cooling processes for ES-85-23 (a), -80 (b), -100 (c) and -120 (d). Each critical gel temperature, at which G' and G'' [25] are comparable, is also shown in Fig. 5. The viscoelastic functions of all TPUs in the heating and cooling processes were quite different. This result was similar to that reported by Yoon et al. [13]. In the heating process, G' values decreased quickly, while G'' values decreased gradually for all TPUs up to 215 °C. In the cooling process, G' values increased quickly and G'' values increased gradually until ca. 150 °C for all TPUs. It took ca. 45 min for the temperature sweep experiment during the heating and cooling processes, including preparation time for measurements. To evaluate the change of the M_w under an isothermal dynamic condition, the time sweep experiments at each temperature were conducted for 50 min. Fig. 6 shows the time evolution of dynamic viscosity for ES-85-23 at temperatures ranging from 180 to 225 °C under a nitrogen atmosphere. The viscosity decreased with increasing time and measurement temperature, and was strongly dependent on the temperature. The times approaching equilibrium values at measurement temperature above 205 °C were longer than those below 190 °C. These results imply that the molecular weight of TPUs decreased at 200 °C or above because of the dissociation reaction of urethane bonds. The inset in Fig. 6 shows M_ws after the time sweep measurements as a function of the rheological measurement temperature. The M_w values after applying dynamic strain at higher temperature in the melt state decreased with increasing measurement temperature. The initial M_w of ES-85-23 before the experiment was ca. 180×10^3, while those magnitudes after the experiments at 190 and 215 °C were ca. 120×10^3 and ca. 90×10^3,

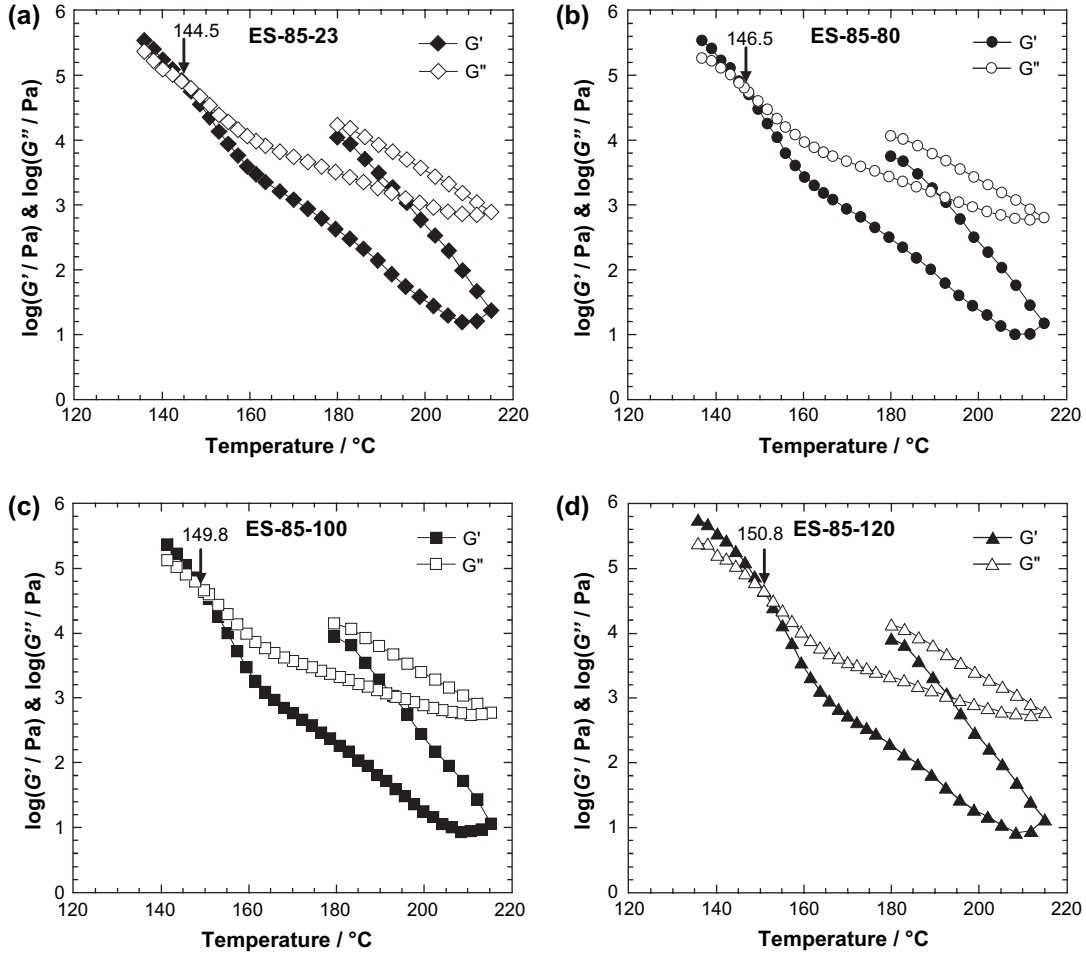

Fig. 5. Temperature dependence of the dynamic storage modulus (G') and dynamic loss modulus (G'') during both the heating and cooling processes at a frequency of 0.628 rad s^{-1} for ES-85-23 (a), ES-85-80 (b), ES-85-100 (c) and ES-85-120 (d).

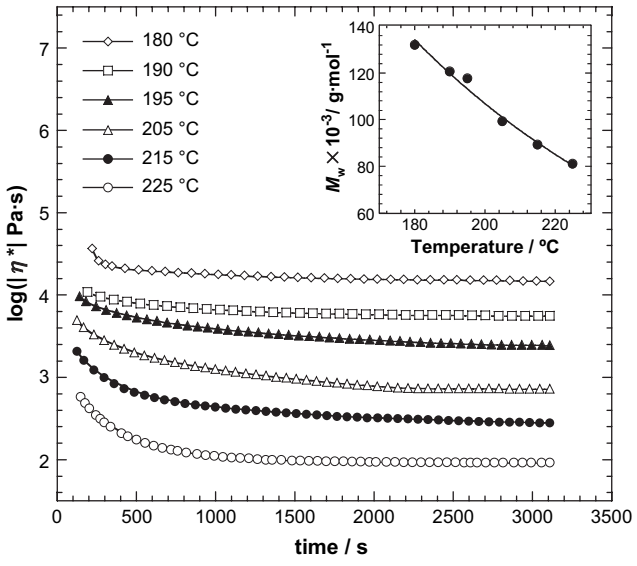

Fig. 6. Variations of dynamic viscosity with time for ES-85-23 at temperatures ranging from 180 to 225 °C. The inset shows the weight-average molecular weight after the time sweep experiments as a function of the rheological measurement temperature.

respectively. These results clearly suggest that a dissociation reaction occurred during time sweep experiments [14]. Thus, the hysteresis behavior of the visoelastic functions in Fig. 5 was attributed to the decreases in M_w during the rheological measurements and change of the micro-phase-separated structure. In addition, we calculated the apparent activation energy of flow (E_a) and true activation energy of flow (E_η) using the equilibrium complex viscosity of ES-85-23 at 3000 s according to the equation proposed by Lu and Macosko et al. [15]. When ΔH_{deg} was assumed to be 58 kJ/mol reported by Hentschel and Münstedt [14], E_a and E_η of ES-85-23 were 215 and 116 kJ/mol, respectively. These activation energies were close to 233 kJ/mol of E_a and 131 kJ/mol of E_η reported by them [14]. Their TPU was composed of poly(tetramethylene ether glycol) with M_n of 800, MDI and BD as the hard segment and its hard segment content (HSC) was ca. 34 wt%. The difference in E_a and E_η reported by Macosko et al. [15] and our values was attributed to HSC, because they used the TPU composed of MDI and hexanediol only.

In Fig. 5, rapid increases in G' were observed below 160 °C, and G' coincided with G'' around 144–150 °C for all TPUs. The T_{cg} increased with increasing annealing temperature, while M_ws of the TPUs decreased after the rheological

measurements. To investigate the mechanism of the rapid increases in G', the start temperature for crystallization of the hard segments ($T_{c,\ start}$) during cooling process was measured by DSC using the same specimens. The $T_{c,\ start}$ values of ES-85-23, -80, -100 and -120 were 147.6, 148.3, 151.1 and 152.2 °C, respectively. Although the cooling rate in the DSC measurements was different from that in the rheological measurements, it is conceivable that the steep increase in G' below 160 °C was attributed to the crystallization of the hard segments. Fig. 7 shows the relationship between $T_{c,\ start}$ and T_{cg}. T_{cg} changed almost linearly with $T_{c,\ start}$. Seymour et al. [3], Koberstein et al. [12] and Turner et al. [26] reported that hydrogen bonded N–H absorbance for MDI- and BD-based polyurethane remained around 200–220 °C in FT-IR measurement. Hence, the increase in T_{cg} with increasing annealing temperature in this study might be attributed to the fact that the residual hard segment domains played as a nuclei for crystallization during the cooling process. From these results, the rheological measurement is a useful technique even for the evaluation of the aggregation state of the hard segment domains in TPUs.

The effects of the micro-aggregation structure on the uniaxial elongational viscosity ($\eta_E(t)$) of TPUs were investigated using a Meissner type extensional rheometer. Fig. 8 shows the time dependence of $\eta_E(t)$ with various strain rates of 0.01, 0.1 and 1.0 s^{-1} at 175, 180 and 190 °C for ES-85-23 (a), -80 (b), -100 (c) and -120 (d). The solid lines in Fig. 8 represent $3\eta(t)$ at 180 and 190 °C, where $\eta(t)$ is the shear stress growth coefficient in the linear viscoelastic region calculated from the shear storage modulus ($G'(\omega)$) and loss modulus ($G''(\omega)$) using an approximate equation proposed by Osaki et al. [27]. The equation is as follows:

$$\eta(t) = t[G''(\omega) + 1.12G'(0.5\omega) - 0.200G'(\omega)]_{\omega=1/t} \quad (2)$$

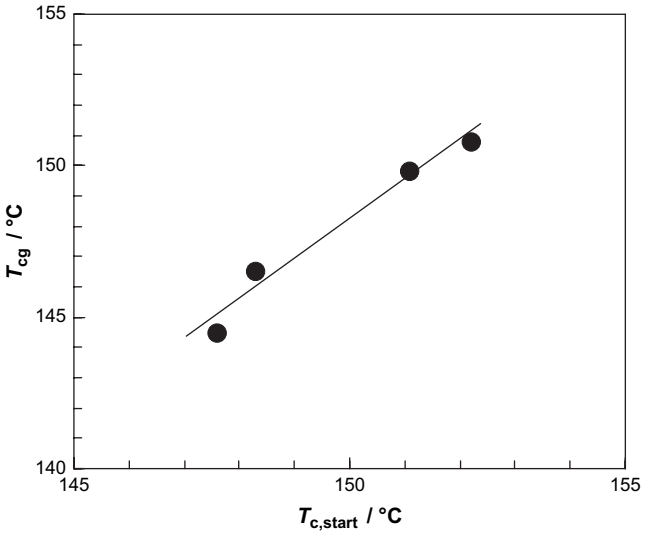

Fig. 7. Relationship between the start temperature for crystallization of the hard segments ($T_{c,\ start}$) obtained from DSC measurements and the temperature at critical gel point (T_{cg}) obtained from the dynamic temperature sweep measurements.

Where, ω is an angular frequency. The experimental data in shear and uniaxial extension for a poly(isobutylene) melt and a polystyrene melt were reported by Demarmels et al. [28] and Takahashi et al. [29]. These results revealed that $\eta_E(t)$ coincided with $3\eta(t)$ at short time region. The time–temperature superposition principle for TPUs was not applied, using the dynamic frequency sweep data measured at temperatures ranging from 180 to 215 °C with a frequency ranging from 0.1 to 100 rad s^{-1}. Therefore, $3\eta(t)$ at 180 and 190 °C was calculated from $G'(\omega)$ and $G''(\omega)$ measured only at the measurement temperature of $\eta_E(t)$, but that at 175 °C could not be calculated owing to the gel state at this temperature. The behavior of $\eta_E(t)$ was significantly different in the specimens. The temperature, at which $\eta_E(t)$ of the TPUs can be measured, was limited. Below 170 °C, the specimens were too hard to clip properly, as can be easily speculated by DSC thermograms (Fig. 1). On the other hand, above 200 °C, the measurement was quite difficult because the specimens loosened due to melting. Thus, we carried out measurements at 175, 180 and 190 °C. As shown in Fig. 8, the strain hardening behavior was observed with increasing time for all TPUs. These strain hardening behaviors were attributed to stretch of the soft segments owing to existence of residual hard segment domains and entanglement. The strain hardening behaviors were also observed at 180 °C, similar to those at 175 °C. In addition, it was obvious that the Trouton ratio of uniaxial elongational viscosity to shear viscosity, could be applied at 180 °C. According to the Doi–Edward's theory [30], when the external rate of strain is high enough for the primitive chain to extend, strain hardening behavior or upturn of uniaxial elongational viscosity is expected. In this work, the primitive chain was attributed not only to entanglement of the polymer chain but also to aggregation of the hard segments. Upturns of $\eta_E(t)$ measured at 180 °C were observed during a longer period of time than those observed at 175 °C. These results suggest that the residual hard segment domains at 180 °C slightly melted in comparison with that at 175 °C. Sharp upturns of $\eta_E(t)$ after gradual decreases in $\eta_E(t)$ during longer periods were observed with time, in particular, for ES-85-23 and -80 at the strain rate of 0.01 s^{-1}. This aspect will be discussed later in relation to data illustrated in Fig. 11. On the contrary, upturns of $\eta_E(t)$ measured at 190 °C were not observed even at a strain rate of 1.00 s^{-1}. This is attributed to the fact that there were no hard segment domains at 190 °C, which are necessary to stretch the soft segments. Moreover, $3\eta(t)$ calculated from the G' and G'' obtained from the dynamic frequency sweep measurements at 190 °C was lower than $\eta_E(t)$ at 190 °C. The measurement time for $\eta_E(t)$ at 190 °C was necessary for ca. 240 s, whereas the time of the rheological measurement at 190 °C was for ca. 800 s. The reason for the disagreement between $3\eta(t)$ and $\eta_E(t)$ is attributed to a decrease in M_w at a higher temperature because the time spent for the rheological measurement was longer than that for uniaxial elongation measurement.

Fig. 9 shows time dependence of the non-linear parameter (λ_n) of uniaxial elongational viscosity measured at 175 °C with strain rates of 0.01, 0.1 and 1.0 s^{-1} (a), and those at

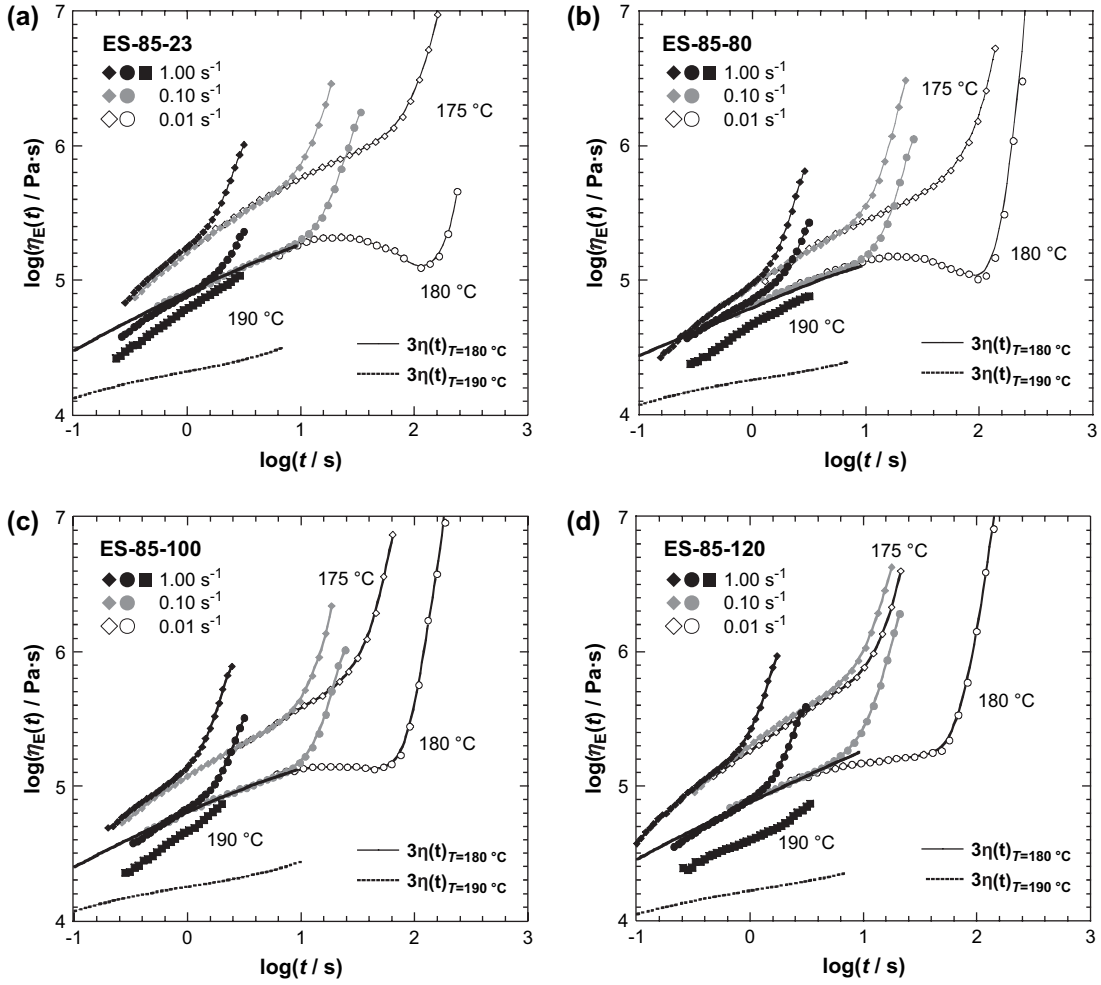

Fig. 8. Time dependence of uniaxial elongational viscosity ($\eta_E(t)$) with strain rates of 0.01, 0.1 and 1.0 s^{-1} at 175, 180 and 190 °C for ES-85-23 (a), ES-85-80 (b), ES-85-100 (c) and ES-85-120 (d).

180 °C with the strain rate of 0.1 and 1.0 s^{-1} (b). λ_n was calculated from the equation proposed by Koyama et al. [31]

$$\lambda_n = \frac{\eta_E(t)_{\text{non-linear}}}{\eta_E(t)_{\text{linear}}} \tag{3}$$

The regions of $\eta_E(t)_{\text{non-linear}}$ and $\eta_E(t)_{\text{linear}}$ were defined as shown in Fig. 10. λ_n at 180 °C and a strain rate of 0.01 s^{-1} could not be calculated, since it was difficult to determine $\eta_E(t)_{\text{linear}}$, due to the gradual decrease in $\eta_E(t)$ above 16 s. Upturns of λ_n were observed clearly at shorter times with increasing strain rate at 175 and 180 °C and the upturn time of the λ_n at 175 °C was shorter than that at 180 °C. This is attributed to a difference in the content of residual hard segment domains at an operating temperature.

Fig. 11 shows time dependence of $\eta_E(t)$ normalized with $\eta_E(t)$ at $t = 6$ s. Measurement conditions were 180 °C and a strain rate of 0.01 s^{-1}. As λ_n could not be calculated owing to the decrease in $\eta_E(t)$ above 16 s, we calculated the normalized $\eta_E(t)$ using the $\eta_E(t)$ at $t = 6$ s as the minimum value within a linear region of $\eta_E(t)$. The decreasing normalized $\eta_E(t)$ was observed above 16 s for the ES-85-23 and -80, but not observed for the ES-85-100 and -120. However, upturns of the normalized $\eta_E(t)$ for ES-85-23 and -80 were observed above 100 s. Gradual decreases in $\eta_E(t)$ above 16 s might not be related to a decrease in M_w of TPUs during the rheological measurement because the M_ws for all TPUs before the measurement were almost same. A similar gradual decrease in $\eta_E(t)$ with time after increasing the viscosity was reported using poly(styrene-*block*-butadiene-*block*-styrene) triblock copolymer (SBS) by Takahashi et al. [32,33]. They concluded that the block copolymerized structure decreased melt elasticity under elongational and shear deformation. As a result, the uniaxial elongational viscosity for SBS did not change after the gradual viscosity increase because the lack of melt elasticity in SBS melt was caused by orientation of the lamellar structure towards the stretched direction during deformation.

In our study, a gradual decrease in $\eta_E(t)$ was observed according to a decrease in the annealing temperature, in other words, in relation to the micro-aggregation of the hard segments. Although these results seemed attributable to differences in aggregation state and the orientation of the hard

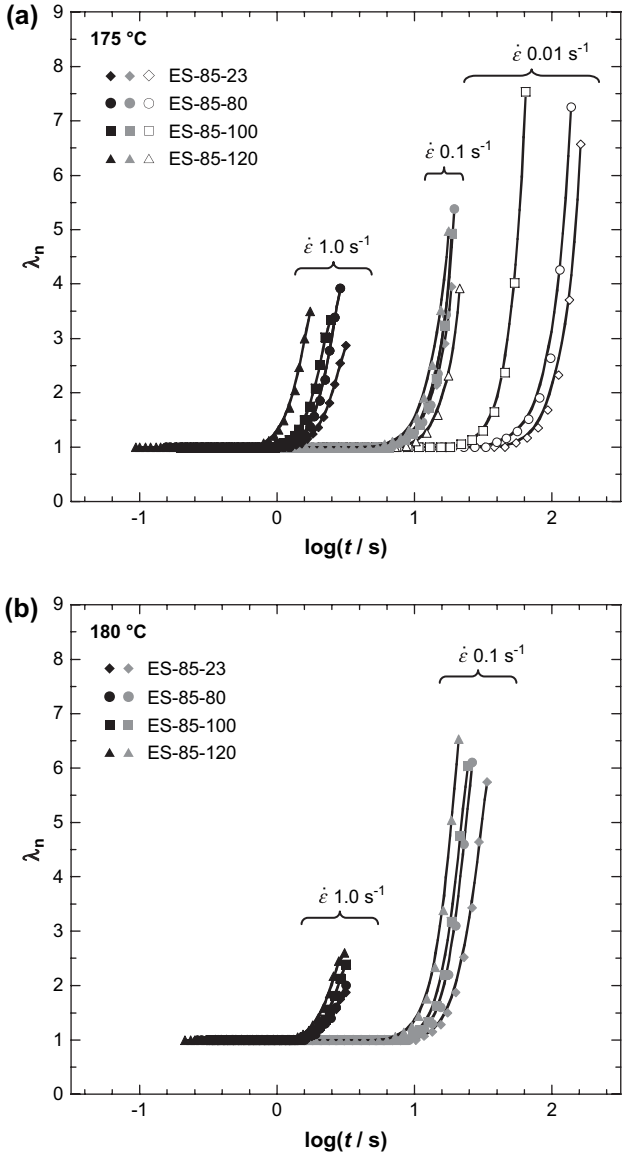

Fig. 9. Time dependence of the non-linear parameter (λ_n) of uniaxial elongational viscosity measured at 175 °C with strain rates of 0.01, 0.1 and 1.0 s^{-1} (a), and those at 180 °C with strain rates of 0.1 and 1.0 s^{-1} (b).

segment domains towards the stretching direction, the reason that $\eta_E(t)$ once decreased before strain hardening is not understood in detail.

4. Conclusions

The effects of the molecular aggregation structure on the rheological properties of MDI- and BD-based TPU were investigated. We prepared four specimens with different molecular aggregation structures by changing the annealing temperature. The micro-phase separation of the TPUs became stronger with increasing annealing temperature. The degree of the micro-phase separation strongly influenced the sol-to-gel transition temperature and the strain hardening of uniaxial elongational viscosity. The sol–gel transition temperature increased with

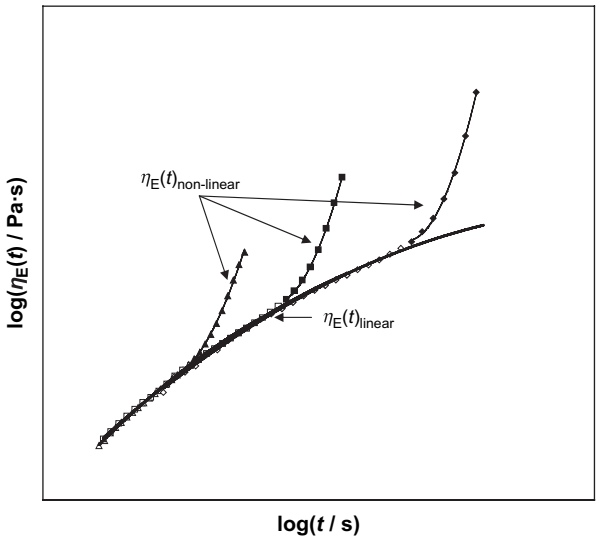

Fig. 10. Schematic model for the non-linear uniaxial elongational viscosity and the linear viscosity to calculate the non-linear parameter (λ_n) of uniaxial elongational viscosity.

the increasing degree of micro-phase separation on account of the effect of residual hard segment domains. We firstly clarified that the time at which strain hardening was clearly observed, shifted to the shorter side with the increasing degree of micro-phase separation in the uniaxial elongational viscosity (η_E) measurement. The upturn of η_E was attributed to the residual hard segment domains as well as entanglement of molecules in the TPU at an operating temperature. The results obtained in this study are quite useful for the polymer processing of TPUs demonstrated by extensional flow, illustrated with film casting, tubular film inflation, fiber spinning and blow molding.

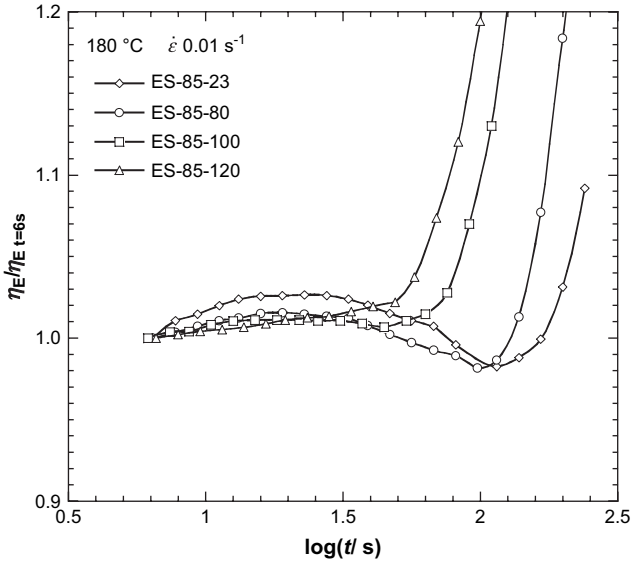

Fig. 11. Normalized uniaxial elongational viscosity ($\eta_E/\eta_{E,\ t=6s}$) at 180 °C and a strain rate of 0.01 s^{-1} with uniaxial elongational viscosity obtained at $t = 6$ s.

References

[1] Randall D, Lee S, editors. The polyurethanes book. New York: John Wiley & Sons Press; 2000.
[2] Oertel G, editor. Polyurethane handbook. Munich: Hanser Press; 1994.
[3] Seymour RW, Cooper SL. Macromolecules 1973;6:48–53.
[4] Koberstein JT, Russell TP. Macromolecules 1986;19:714–20.
[5] Koberstein JT, Leung LM. Macromolecules 1986;19:706–13.
[6] Koberstein JT, Galambos AF. Macromolecules 1992;25:5618–24.
[7] Hu W, Koberstein JT. J Polym Sci Part B Polym Phys 1994;32:437–46.
[8] Phillips RA, Cooper SL. J Polym Sci Part B Polym Phys 1996;34: 737–49.
[9] Leung LM, Koberstein JT. J Polym Sci Polym Phys Ed 1985;23:1883–913.
[10] Van Borgart JWC, Bluemke DA, Cooper SL. Polymer 1981;22:1428–38.
[11] Hesketh TR, Van Borgart JWC, Cooper SL. Polym Eng Sci 1980; 20:190–7.
[12] Koberstein JT, Gancarz I. J Polym Sci Part B Polym Phys 1986; 24:2487–98.
[13] Yoon PJ, Han CD. Macromolecules 2000;33:2171–83.
[14] Hentschel T, Münstedt H. Polymer 2001;42:3195–203.
[15] Lu QW, Hernandez-Hernandez ME, Macosko CW. Polymer 2003; 44:3309–18.
[16] Cossar S, Nichetti D, Grizzuti N. J Rheol 2004;48:691–703.
[17] Velankar S, Cooper SL. Macromolecules 1998;31:9181–92.
[18] Velankar S, Cooper SL. Macromolecules 2000;33:382–94.
[19] Velankar S, Cooper SL. Macromolecules 2000;33:395–403.
[20] Das S, Yilgor I, Yilgor E, Inci B, Tezgel O, Beyer FL, et al. Polymer 2007;48:290–301.
[21] Clayden NJ, Howick C. Polymer 1993;34:2508–15.
[22] Saotome K, Komoto H. J Polym Sci A-1 1967;5:119–26.
[23] Chamberlin Y, Pascault JP, Letoffe M, Claudy P. J Polym Sci A 1982;20:1445–56.
[24] Yang G, Chen Q, Wang Y, Yang C, Wu X. J Mole Struct 1994;323:209–14.
[25] Winter HH, Chambon F. J Rheol 1986;30:367–82.
[26] Christenson CP, Harthcock MA, Meadows MD, Spell HL, Howard WL, Creswick MW, et al. J Polym Sci Part B Polym Phys 1986;24:1401–39.
[27] Osaki K, Murai N, Bessho N, Kin BS. Nihon Reoroji Gakkaishi 1976;4:166–9.
[28] Demermels A, Meissner. J Colloid Polym Sci 1986;264:829–46.
[29] Takahashi M, Isaki T, Takigawa T, Masuda T. J Rheol 1993;37:827–46.
[30] Doi M, Edwards SF, editors. The theory of polymer dynamics. Oxford: Clarendon Press; 1986 [chapter 7].
[31] Koyama K, Ishizuka O. Nihon Reoroji Gakkaishi 1985;13:93–100.
[32] Takahashi T, Toda H, Minagawa K, Iwakura K, Koyama K. In: Proceeding of the Pacific conference on rheology and polymer processing (PCR'94); 1994. p. 134–5.
[33] Takahashi T, Toda H, Minagawa K, Takimoto J, Iwakura K, Koyama K. J Appl Polym Sci 1995;56:411–7.